NIH Public Access
Author Manuscript
Mech Dev. Author manuscript; available in PMC 2009 July 1.

Published in final edited form as:
Mech Dev. 2008 July ; 125(7): 601–616.

bHLH-PAS family transcription factor methoprene-tolerant plays a key role in JH action in preventing the premature development of adult structures during larval-pupal metamorphosis

R. Parthasarathy, **Anjiang Tan**, and **Subba R. Palli**
Department of Entomology, College of Agriculture, University of Kentucky, Lexington, KY 40546

Abstract

The biological actions of juvenile hormones are well studied; they regulate almost all aspects of an insect's life. However, the molecular actions of these hormones are not well understood. Recent studies in the red flour beetle, *Tribolium castaneum*, demonstrated the utility of this insect as a model system to study JH action. These studies confirmed that the bHLH-PAS family transcription factor, methoprene-tolerant (TcMet,) plays a key role in JH action during larval stages. In this study, we investigated the role of TcMet in JH action during larval-pupal metamorphosis. The phenotypes of TcMet RNAi insects shared similarity with the phenotypes of some allatectomized lepidopteran larvae that were attempting to undergo precocious larval-pupal metamorphosis. Knocking-down TcMet during the final instar also disrupted larval-pupal ecdysis, resulting in the development of adultoid underneath the larval skin. However, the loss of TcMet did not completely block remodeling of internal tissues such as midgut. *T. castaneum* larvae injected with TcMet dsRNA demonstrated a resistance to a JH analog (JHA), hydroprene, irrespective of time and route of application. Knocking-down TcMet also caused down regulation of JH-response genes, JHE and Kr-h1 suggesting that TcMet might be involved in the expression of these genes. Based on the phenotype, gene expression, and JHA action studies in TcMet RNAi insects, this study concludes that Met plays a key role in JH action for preventing the premature development of adult structures during larval-pupal metamorphosis.

Keywords

juvenile hormone; RNAi; metamorphosis; ecdysis; gene expression; JH analogs; bHLH-PAS; midgut

1. Introduction

Juvenile hormones (JH) regulate a broad array of insect developmental and physiological processes, yet the molecular mechanism of these hormones is not well understood (Riddiford, 1985; 1994; Nijhout and Wheeler, 1982). JH is present during the larval stages of almost all insects; its role during larval development is to maintain 'status quo'; allowing larval molting and preventing metamorphosis (Williams, 1961; Truman and Riddiford, 1999; 2002). Absence of JH during rise in 20-hydroxyecdysone (20E) levels (commitment peak) at the end of feeding stage of the final instar is believed to allow commitment to undergo metamorphosis (Riddiford

*Corresponding Author, Phone: 859 257 4962, Fax: 859 323 1120, Email: RPALLI@EMAIL.UKY.EDU.

Publisher's Disclaimer: This is a PDF file of an unedited manuscript that has been accepted for publication. As a service to our customers we are providing this early version of the manuscript. The manuscript will undergo copyediting, typesetting, and review of the resulting proof before it is published in its final citable form. Please note that during the production process errors may be discovered which could affect the content, and all legal disclaimers that apply to the journal pertain.

NIH-PA Author Manuscript
NIH-PA Author Manuscript
NIH-PA Author Manuscript

NIH-PA Author Manuscript

NIH-PA Author Manuscript

NIH-PA Author Manuscript

et al. 1986; 2003). Application of exogenous JH during or prior to commitment stage blocked metamorphosis in insects belonging to Lepidoptera and Coleoptera (Truman et al. 1974; Riddiford, 1978; Kostyukovsky et al. 2000) by modulating the 20E-induced gene expression (Zhou et al. 1998; Hiruma et al. 1999; Wu et al. 2006, Parthasarathy and Palli, 2007).

However, JH reappears at the end of the final instar after the commitment peak of 20E (Baker et al. 1987; Riddiford, 1994); its critical role is thought to allow normal larval-pupal transition by preventing precocious adult development. This was verified by removing the source of JH, corpora allata, during the final instar of various insects (Truman and Riddiford, 2002). The most extreme response was observed only in *Cecropia* silkworm where allatectomized larvae transformed into pupae that had extensive adult characters (Williams, 1961). Hence, the requirement for JH in the larval-pupal transition remains unclear as the response of allatectomized insects varied dramatically. Most of the previous studies were focused on the 'status quo' role of JH during larval development or its modulatory role during pupal commitment resulting in the lack of our understanding of its important regulatory role during larval-pupal transition where it prevents precocious adult development.

Methoprene-tolerant (Met), a bHLH-PAS domain family transcription factor, reported to be involved in JH action (Wilson and Fabian, 1986; Ashok et al. 1998; Flatt and Kawecki, 2004), seems to be an ideal candidate to study JH action. Although the Met locus was identified and genetically characterized from mutagenic screening of *Drosophila melanogaster* that were resistant to juvenile hormone analog (Wilson and Fabian, 1986), it did not serve the purpose of unraveling the mechanisms of JH action in *D. melanogaster* metamorphosis for various reasons. First of all, *D. melanogaster* is insensitive to exogenous JH during pre-adult development except for abdominal histoblasts (Ashburner, 1970; Postlethwait, 1974; Riddiford and Ashburner, 1991). Genetic studies on the Met locus showed that Met allele is amorphic and may not be mutable further to affect viability, development and reproduction (Wilson, 1996) leading to the unexpected viability of *Met* mutant (Wilson and Ashok, 1998). The functional redundancy of a closely related gene, germ-cell expressed (gce), whose protein product dimerizes with Met in a JH-dependent manner (Moore et al. 2000; Wang et al. 2007; Godlewski et al. 2006), has been proposed to explain the unexpected viability of *Met* mutants.

A search for Met homologs in other insects identified a single ortholog of *D. melanogaster* Met and gce in lower dipteran mosquitoes (Wang et al. 2007) and coleopteran beetles (Konopova and Jindra, 2007). Of these, beetles might offer the better model for JH studies because of their high sensitivity to JH (Kostyukovsky et al. 2000; Parthasarathy and Palli, unpublished). Recently, Met was shown to mediate "the status quo" action of JH during the early larval instars of *Tribolium castaneum* (Konopova and Jindra, 2007). However, this study did not provide evidence for Met action in all normal JH functions (Willis, 2007), as this study primarily focused on the role of Met in JH action during larval-larval molting and the anti-metamorphic effect of JHA in Met deficient insects during the pupal stage. The role of Met in JH action to prevent premature adult development during larval-pupal metamorphosis is still unknown.

RNA interference (RNAi) works well in *T. castaneum* (Arakane et al. 2005; Konopova and Jindra, 2007; Parthasarathy et al. 2008; Tan and Palli, 2007; Suzuki et al. 2008). In this study, we utilized RNAi to determine the precise role of JH/TcMet during larval-pupal metamorphosis. Knocking–down TcMet disrupted larval-pupal ecdysis and induced precocious adult development upon partial ecdysis. Also, TcMet deficient final instar larvae were resistant to ectopic application of JH analog, hydroprene, during larval-pupal metamorphosis. Silencing of TcMet resulted in a decrease in the expression of some JH-response genes. However, knock-down of TcMet did not completely block remodeling of internal tissues such as midgut. Taken together, these data provide evidence for the role of

NIH-PA Author Manuscript

NIH-PA Author Manuscript

NIH-PA Author Manuscript

TcMet and JH at the end of the final instar to ensure normal pupal development by preventing precocious adult development.

2. Results

2.1. Expression profiles of TcMet mRNA during metamorphosis

The mRNA levels of TcMet were determined in the whole body as well as in the midgut tissue collected at 12 h intervals during the final instar and pupal stages. The expression of TcMet mRNA in the whole body was high during the early hours of the final instar and declined to lower levels thereafter. These low levels were maintained until 12 h after the larvae entered the quiescent stage (Fig. 1A). The TcMet mRNA levels started increasing again beginning at 12 h after the larvae entered the quiescent stage and reached the maximum levels at the end of the quiescent stage. These levels remained high until 12 h after ecdysis into the pupal stage (AEPS). The expression of TcMet then decreased and remained low throughout the pupal stage except for a small increase prior to adult emergence. In the midgut, the TcMet mRNA levels increased beginning at 12 h after ecdysis into the final instar (AEFI) and these higher levels were maintained until 84 h AEFI.(Fig. 1B). The TcMet mRNA levels then decreased and reached the minimum levels when the larvae entered the quiescent stage. The TcMet mRNA levels increased again beginning at 24 h after the larvae entered the quiescent stage and reached the maximum levels by the larval-pupal ecdysis. The TcMet mRNA levels decreased soon after ecdysis into the pupal stage and remained low during the pupal stage.

2.2. Effect of TcMet knockdown on gene expression

To determine the effectiveness of dsRNA in knocking-down TcMet gene, qRT-PCR was used to quantify TcMet mRNA levels in TcMet dsRNA injected insects and control insects injected with *malE* dsRNA. The dsRNA injections were done at 24 h AEFI and the insects were sampled at 24, 72, and 120 h after injection. The expression of TcMet mRNA was two-fold lower at 24 h and 72 h after injection in TcMet dsRNA injected insects when compared to its levels in control insects injected with *malE* dsRNA. However, the highest reduction in TcMet mRNA levels (10-fold) was observed at 120 h after injection of dsRNA. To determine the effect of knock-down of TcMet on the expression of JH-response genes, the mRNA levels of two known JH-response genes, JHE and Kr-h1 (Kethidi et al. 2004; Minakuchi et al. 2008) were quantified in insects injected with TcMet or *malE* dsRNA. In the insects injected with TcMet dsRNA, the mRNA levels of JHE and Kr-h1 were three-fold lower than in control larvae injected with *malE* dsRNA suggesting that TcMet directly or indirectly regulates the expression of JHE and Kr-h1 (Fig. 2B).

The effect of knock-down of TcMet on JH regulation of JHE and Kr-h1 was determined by *in vitro* organ culture and qRT-PCR. The mRNA levels of TcMet, JHE and Kr-h1 were compared between tissues dissected from the insects injected with TcMet or *malE* dsRNA (control) and cultured in medium containing DMSO or JH III. In the tissues dissected from control insects, TcMet and Kr-h1 showed higher levels of mRNA even after exposure to DMSO alone and the mRNA levels were not induced further after culturing in JH III containing medium (Fig. 2C). In control insects, the mRNA level of JHE was induced by 10-fold after culturing the tissues in JH III containing medium when compared to the levels in tissues cultured in DMSO containing medium (Fig. 2C). However, the expression levels of all three genes were lower in TcMet dsRNA injected insects in both DMSO alone and JH III treatment when compared to control insects, suggesting that TcMet is required for expression of JHE and Kr-h1 genes (Fig. 2C).

NIH-PA Author Manuscript

NIH-PA Author Manuscript

NIH-PA Author Manuscript

2.3. TcMet RNAi induces precocious adult development and disrupts larval-pupal ecdysis

Injection of TcMet dsRNA at 24 h AEFI caused disruption of larval-pupal ecdysis and precocious development of some structures (compound eyes, antennae, legs, and wings) similar to those seen in adult insects (Fig. 3A, a–e, k, l, n, o). TcMet RNAi insects showed the development of ommatidia (photoreceptors of compound eyes) beneath the larval cuticle at 108 h after injection (Fig. 3A, a). Sclerotization of head and thoracic regions was observed at 120 h after injection (Fig. 3A, b). Initiation of ecdysis was noticed at 144 h after injection, the larval cuticle began detaching from the body. The forewings pads which were sclerotized beneath the larval cuticle were evident (Fig. 3A, c). Ecdysis of larval cuticle continued at 168 h after injection; and the separation of the larval cuticle from the head and thoracic regions of the body was evident at this time (Fig. 3A, d). Ecdysis of larval cuticle was partially completed with portions of exuviae were still attached to the abdominal regions at 176 h after injection (Fig. 3A, e). The developmental progression of control insects injected with *malE* dsRNA at 24 h AEFI was normal (Fig. 3A, f–j). The final instar larvae entered the quiescent stage at 72 h after injection and proceeded to become pupae at 120 h after injection (data not shown). The development of compound eyes, adult antennae, adult legs and sclerotization of elytra occurred during the pupal stage (Fig. 3g–i) and the pupae developed into pharate adult by 220 h after injection (Fig. 3A, j).

TcMet RNAi insects showed distinct adultoid characters beginning at 176 h after injection (Fig. 3A, k & l). The head region had sclerotized antennae and well developed compound eyes similar to those seen in adults (Fig. 3A, k & l). The pronotum was well developed and sclerotized resembling that in adults. The elytra, though short, were sclerotized similar to those in adults. The legs and thoracic sternal plates were sclerotized resembling to those in adults (Fig. 3A, l). The control insects injected with *malE* dsRNA at 176 h after injection were in the pupal stage and showed unsclerotized antennae, pronotum, elytra, legs and thoracic sternal plates, and pupal abdominal cuticle bearing gin-traps (Fig. 3A, m). When the larval skin was physically removed from the abdomen of the TcMet RNAi insects at 120 h after injection, the pupal cuticle was observed underneath the larval cuticle (Fig. 3A, n). At higher magnification, the pupal cuticle developed underneath the unshed larval cuticle had gin-traps and distinct pupal urogomphi (Fig. 3A, o). In light of these phenotypes, we conclude that knockdown of TcMet during the final instar disrupts and delays larval-pupal ecdysis and pupae develop underneath the unshed larval cuticle on par with the control insects. However, TcMet knock-down induced precocious adult characters in structures differentiating from the imaginal cells in the head and thoracic regions while retaining pupal characters in the abdominal epidermis. As a result, TcMet RNAi insects show adultoid characters upon incomplete ecdysis.

In order to study the structures of organs developed after TcMet RNAi in detail, these structures were observed under a scanning electron microscope (SEM). Injection of TcMet dsRNA was done at 24 h AEFI and insects that showed phenotypes at 176 h after injection were analyzed (Fig. 3B, a–h). The mouthparts showed well developed maxillary and labial segments with palpi (Fig. 3B, a); the labrum was concealed, unlike in pupae where it is distinct; the incisors of mandibles were extended to overlap like those seen in adults; in pupae a distinct gap exists between the mandibles (see Fig. 3A, h & i). The compound eyes were well developed similar to those seen in adults with several rows of ommatidia (Fig. 3B, b). The antennae were well developed and similar to those seen in adults with distinct flagellar segments (Fig. 3B, c). The forewing (elytra) was short and undeveloped while the hindwing was normal (Fig. 3B, d). The legs were short, stout and stumped while the tarsal segments (though less differentiated) terminating in a pair of claws were similar to those seen in adults (Fig. 3B, e). The abdominal region showed the pupal cuticle with the presence of gin-traps and attached larval exuvium (Fig. 3B, f). When the exuvium was physically removed, the abdomen had well developed

NIH-PA Author Manuscript

NIH-PA Author Manuscript

NIH-PA Author Manuscript

male genital papillae (Fig. 3B, g) and distinct pupal urogomphi (Fig. 3B, h). For a comparison to wild-type larval, pupal, and adult counterparts, please refer to Parthasarathy et al. (2008).

The unshed larval cuticle was physically removed from the head, thorax and terminal abdominal regions of TcMet RNAi insects at 120 h after injection and SEM images were recorded. The head and thoracic regions showed smooth cuticle devoid of sensory bristles (Fig. 4B, a). The larval cuticle had long setae while the pupal cuticle had short setae (Fig. 3C, c). Both of these types of setae and typical adult sensory bristles were absent in the cuticle present in the head and thoracic regions underneath the unshed larval cuticle (Fig. 3C, a). The abdominal regions showed pupal cuticle with distinct gin-traps (Fig. 3C, a–d) suggesting that the abdominal cuticle underneath the unshed larval cuticle was mostly pupal. The phenotypes of TcMet RNAi insects are compared with the descriptions of periodic developmental events of control insects (Table 1).

2.4. Knock-down of TcMet overcomes anti-metamorphic effect of JHA during larval-pupal metamorphosis

TcMet was shown to confer insensitivity to ectopic JH when applied during the pupal stage (Konopova and Jindra, 2007). To determine whether TcMet plays a similar role during larval-pupal metamorphosis, three different experimental regimes were set up.

Experiment I—TcMet or *malE* dsRNA was injected at 24 h AEFI and the insects were fed on diet containing acetone or hydroprene immediately (Fig. 4a–d). All control larvae that were injected with *malE* dsRNA and fed an acetone diet successfully pupated (Fig. 4a). All control larvae that were injected with *malE* dsRNA and fed a hydroprene diet underwent supernumerary larval molt (Fig. 4b). The larvae injected with TcMet dsRNA and fed an acetone diet showed typical TcMet RNAi phenotype (Fig. 4c, 97%), while the larvae injected with TcMet dsRNA and fed a hydroprene diet underwent precocious metamorphosis (Fig. 4d, 93%) escaping supernumerary larval molt seen in the control larvae (Fig. 4b).

Experiment II—The insects were fed an acetone or hydroprene diet beginning at 24 h AEFI and subjected to dsRNA injections at 96 h AEFI (Fig. 4e–h). The larvae fed a hydroprene diet underwent first supernumerary larval molt irrespective of dsRNA injected. However, all the control larvae injected with *malE* dsRNA and fed hydroprene underwent second supernumerary larval molt (Fig. 4f); while 87% of the larvae injected with TcMet dsRNA and fed a hydroprene diet underwent precocious metamorphosis (Fig. 4h) after the first supernumerary larval molt, avoiding the second supernumerary larval molt as seen in the control larvae (Fig. 4f). All the control larvae injected with *malE* dsRNA and fed an acetone diet became adults (Fig. 4e); while 87% of larvae injected with TcMet dsRNA and fed an acetone diet showed TcMet RNAi phenotypes (Fig. 4g).

Experiment III—The insects were injected with dsRNA at 24 h AEFI and administered acetone or hydroprene topically at 96 h AEFI (Fig. 4i–l). 97% of control larvae injected with *malE* dsRNA and received acetone became pharate adults (Fig. 4i); while the larvae that received hydroprene died during the pupal stage. Of those, 67% of pupae showed second pupal cuticle formation when the first pupal abdominal cuticle was physically removed (Fig. 4j). Both larval groups that were injected with TcMet dsRNA and applied with either acetone or hydroprene showed precocious metamorphosis (Fig. 4k & l). These data show that silencing of TcMet during the final instar renders resistance to ectopic application of hydroprene irrespective of time and route of application.

NIH-PA Author Manuscript

NIH-PA Author Manuscript

NIH-PA Author Manuscript

2.5. TcMet RNAi does not completely block remodeling of internal tissue, midgut

We investigated the role of TcMet in the remodeling of internal tissue such as midgut. Midgut remodeling occurs during the larval-pupal metamorphosis where larval cells undergo programmed cell death (PCD), and the intestinal stem cells (ISCs) undergo proliferation and differentiation to form pupal/adult midgut. Also, a few ISCs proliferate and evaginate as crypts during the middle of the pupal stage (Parthasarathy and Palli, 2008).

Cross-sections (10 μm, thick) were taken from midguts dissected from insects injected with TcMet or *malE* (control) dsRNA at two different time points: 120 h after injection (quiescent stage) and 176 h after injection (by this time, TcMet RNAi insects undergo incomplete ecdysis and show adultoid characters). These cross-sections were stained with nuclear dye, DAPI to identify different cell types: larval cells are large, polyploid; ISCs are small, diploid. By 120 h after injection, the midgut of the control insects had larval cells moved into the lumen and the daughters of ISCs (differentiating ISCs) were arranged into a single layer to form pupal/adult midgut (Fig. 5A, a). The midguts dissected from TcMet RNAi insects showed similar morphology with respect to the larval cells, but the proliferation and differentiation of ISCs to form pupal/adult midgut is not readily seen. Only a few small diploid cells were seen on the periphery (Fig. 5A, b).

By 176 h after injection, the midgut of the control insects had a single layer of well differentiated pupal epithelial cells which evaginate out as crypts at some places in both anterior and posterior regions of the midgut (Fig. 5A, c). In TcMet RNAi insects, the anterior region of midgut showed large number of differentiated pupal epithelial cells devoid of crypt formation (Fig. 5A, d), while the posterior region showed evagination of crypt-like structures (Fig. 5A, e). However, the crypts were short and stumped when compared to those seen in control midguts. This data suggests that silencing of TcMet during the final instar does not completely block the midgut remodeling events. The differentiation of daughters of ISCs to form pupal gut, evagination of crypts in the anterior regions, and the development of crypts in the posterior regions of midguts were affected when compared to the midguts of control insects.

2.6. Intestinal stem cell proliferation is delayed in TcMet RNAi insects during larval-pupal metamorphosis

The midguts dissected at 96 h and 176 h after injection were subjected to BrdU assay with anti-BrdU and proliferative cells were detected using anti-mouse Texas-Red conjugated secondary antibody (Fig. 5B, a–l). At the beginning of the quiescent stage (96 h after injection), the ISCs that are dividing were detected on the surface of midgut epithelium arranged in the form of cellular nidi interspersed with larval cells in the midguts dissected from both TcMet and *malE* (control) dsRNA (Fig. 6B, a–f). However, the number of dividing ISCs were less in the midguts dissected from TcMet dsRNA injected insects (Fig. 5B, d–e) when compared to those in the midguts dissected from control insects (Fig. 5B, a–b).

At 176 h after injection, the daughters of stem cells in the crypts stained with BrdU were observed at the posterior region of midguts dissected from both TcMet and *malE* (control) dsRNA (Fig. 5B, g–l). However, the number of BrdU positive cells, length and size of crypts in the midguts dissected from TcMet dsRNA insects (Fig. 5B, j–l) were less than those dissected from control insects (Fig. 5B, g–i). These data suggest that proliferation of ISCs is affected in TcMet RNAi insects during larval-pupal metamorphosis and also prior to formation of crypts in the posterior region of midgut during the later stage of development.

2.7. Effect of TcMet RNAi on PCD of larval cells and evagination of crypts

Morphological observations suggested that TcMet may not be involved in the elimination of larval cells by PCD. To confirm these observations, TUNEL assays were performed on cross-

NIH-PA Author Manuscript

NIH-PA Author Manuscript

NIH-PA Author Manuscript

sections of midguts dissected from *malE* (control) and TcMet dsRNA injected insects at 120 h after injection (Fig. 5C, a–d). TUNEL positive larval cells (green) in the lumen of midgut were observed in both control and TcMet knock-down insects indicating that loss of TcMet did not block elimination of larval cells by PCD during the quiescent stage (120 h after injection).

Knock-down of TcMet affected evagination of crypts in the anterior region of midguts as revealed by morphological observation presented in the previous section (see Fig. 5A, d). To determine the proliferation state of pupal epithelial cells in the midguts dissected from TcMet dsRNA injected insects, BrdU assay was performed on cross-sections of midguts dissected at 176 h after injection (Fig. 5C, e–j). The midguts dissected from control insects at 176 h after injection showed evagination of crypts and BrdU positive cells in the crypts (Fig. 5C, e–g). The midguts dissected from TcMet dsRNA injected insects showed BrdU positive cells in the epithelium (Fig. 5C, h–j), which is a condition observed prior to evagination of crypts in the normal insects. These data clearly showed that evagination of crypts in the anterior region of the midgut is slowed-down in TcMet dsRNA injected insects when compared to that in control insects.

2.8. Hormonal regulation of ISCs proliferation in TcMet RNAi insects

To assess the effect of the silencing of TcMet on the hormonal regulation of ISCs in the midguts, *in vitro* assays and BrdU labeling were performed. TcMet or *malE* dsRNA was injected at 24 h AEFI. Midguts dissected at two days after injection were cultured *in vitro* for two additional days. During the incubation, the midguts were exposed to 10 μM concentration of 20E, JH III or 20E + JH III for 24 h. BrdU pulsing was done for 12 h followed by BrdU labeling and detection. Relative fluorescent intensity (RFI) of BrdU positive cells was measured in the midguts. In control midguts, 20E induced cell proliferation (Fig. 5D). DMSO and JH III alone did not show any effect on cell proliferation. However, addition of JH III to 20E suppressed 20E-induced cell proliferation by 50%. Both 20E induction of cell proliferation and JH III suppression of 20E-induced stem cell proliferation were not affected by knocking-down TcMet. This suggests that TcMet may not be directly involved in 20E induction or JH suppression of 20E-induced proliferation of ISCs.

3. Discussion

The rise in JH levels at the end of the final instar is thought to ensure normal larval-pupal transition (Williams, 1961; Kiguchi and Riddiford, 1978; Hiruma, 1980). Little is known about how the JH signal is mediated at the end of larval stage to ensure normal larval-pupal metamorphosis. How a transcription factor, Met mediates this JH signal during larval-pupal metamorphosis in beetles forms the crux of this study. The removal of the source of JH by allatectomy during the final instar induced precocious adult development in a few insects (Truman and Riddiford, 2002), indicating that the endocrine stimulus for normal pupation is the action of 20E in the presence of a low but finite titer of JH. However, the response of allatectomized insects to this hormonal cue varied dramatically among insects tested, with no effect in *Bombyx mori* and *Galleria mellonella* (Bounhiol, 1938; Piepho, 1945) to intermediate or severe effects in *M. sexta*, *Mamestra brassicae* and *H. cecropia* (Williams, 1961; Kiguchi and Riddiford, 1978; Hiruma, 1980).

Met RNAi shows phenotypes of allatectomized insects

In this study, we used the powerful RNAi technique to knock-down the mRNA levels of Met, a transcription factor known to mediate JH action (Ashok et al. 1998; Restifo and Wilson, 1998; Wilson et al. 2006a; 2006b; Konopova and Jindra, 2007), to study its effect on JH-mediated larval-pupal metamorphosis in *T. castaneum*. Interestingly, the apparent effect of

NIH-PA Author Manuscript

NIH-PA Author Manuscript

NIH-PA Author Manuscript

TcMet depletion in the final instar was precocious adult development in structures such as compound eyes, antennae, wings, and legs. These TcMet RNAi phenotypes in beetles are similar to the phenotypes of allatectomized lepidopteran insects (Williams, 1961; Kiguchi and Riddiford, 1978; Hiruma, 1980). Another striking feature of TcMet RNAi is the disruption of larval-pupal ecdysis. The larval-pupal ecdysis was delayed by 2–3 days resulting in the prolongation of the insects in the quiescent stage. As a consequence, the pupal development occurred underneath the larval skin on par with the control insects except for induction of precocious metamorphosis in some structures upon incomplete ecdysis. Similar conditions were observed when TcMet mRNA levels were silenced in early larval instars. TcMet depletion disrupted ecdysis in the subsequent larval molts and induced precocious metamorphosis (Konopova and Jindra, 2007). Additionally, we demonstrate that the silencing of TcMet during the final instar confers resistance to exogenous application of hydroprene (JHA). TcMet knock-down enabled JHA applied insects to undergo precocious metamorphosis by overcoming JHA induction of supernumerary stages irrespective of time or route of application. Similar mechanisms were observed with methoprene (JHA) treated *Met* mutants of *D. melanogaster* (Wilson and Fabian, 1986; Restifo and Wilson, 1998), and TcMet deficient pupae of *T. castaneum* during pupal-adult metamorphosis (Konopova and Jindra, 2007).

Met mediates JH action during larval-pupal metamorphosis

Several lines of evidence suggest that TcMet is involved in JH signaling pathways during larval-pupal metamorphosis. 1. The direct evidence stems from phenotypes of TcMet RNAi insects sharing similarity with the allatectomized phenotypes of final instar of some lepidopteran insects during larval-pupal metamorphosis. 2. Preliminary data on JH titers of *T. castaneum* showed a rise in JH levels at the end of the larval stage coinciding with the prepupal peak of 20E (Parthasarathy et al. 2008 and data not shown), as observed in other holometabolous insects belonging to Diptera (Riddiford, 1993) and Lepidoptera (Baker et al. 1987). Also, TcMet expression levels in the whole body show a peak at the end of the larval stage. This indicates the possibility of TcMet mediating JH action at the end of the larval stage. 3. Gene expression analysis showed a reduction in mRNA levels of JHE and Kr-h1 in TcMet RNAi insects. Also, the induction of JHE by JH III was eliminated in tissues dissected from TcMet RNAi insects. JHE and Kr-h1 are known to be JH-response genes (Kethidi et al. 2004; Minakuchi et al. 2008) indicating that TcMet may directly or indirectly regulate the expression of genes involved in JH signaling pathways. 4. Silencing of TcMet in the final instar conferred resistance to the effects of JHA during larval-pupal metamorphosis, a mechanism considered as the primary evidence of linking Met to JH action in *Drosophila*.

Having shown that TcMet could mediate JH action during larval-pupal metamorphosis, we then analyzed the TcMet RNAi phenotypes from the perspectives of JH action. Close observation of phenotypes through SEM analysis indicated that adult overshoot was observed only in structures such as compound eyes, antennae, wings, and legs belonging to the head and thoracic regions. Most of these structures arise from the imaginal tissues in the final instar. The cuticle of the head and thoracic regions underneath the larval skin of TcMet RNAi insects was smooth and devoid of any external cuticular structures, whereas abdominal cuticle underneath the larval skin was totally pupal with gin-traps, urogomphi and short setae. Similar mechanisms were observed in allatectomized larvae of *H. cecropia* after pupation (Williams, 1961). Why do these differences in response to JH arise between the imaginal tissues and epidermis? It has been argued that cellular determination of final fates prior to production of pupal cuticle of individual tissues varies, resulting in the differential response of allatectomized insects to JH during larval-pupal metamorphosis (Truman and Riddiford, 2002). At least in lepidopteran insects, the responses of imaginal tissues and epidermis to JH vary during metamorphosis (Kiguchi and Riddiford, 1978; Kurushima and Ohtake, 1975; Nijhout, 1975; Riddiford, 1978). The occurrence of pupal commitment of lepidopteran wing discs is much earlier than

NIH-PA Author Manuscript

NIH-PA Author Manuscript

NIH-PA Author Manuscript

the epidermis (Koyama et al. 2004) and pupal commitment of epidermis of *B. mori* occur even in the presence of a small amount of JH (Maramatsu et al. 2008). Both studies have shown that loss of sensitivity of wing discs and epidermal cells to JH completes the commitment process. Application of JHA during the final instar of tenebrionid beetles revealed the commitment period for wings, antennae, eyes, prothorax and tarsi (Connat et al. 1984, Quennedy and Quennedy, 1999). Though we could not directly relate because of the difference in developmental period of *T. castaneum*, the commitment period is likely to occur through the end of the feeding stage (Parthasarathy and Palli, unpublished). Also, unlike early forming wing discs of Lepidoptera, wing discs of beetles are formed only in the final instar.

The differentiation of imaginal tissues could be induced by the presence of JH, whereas abdominal epidermis does not respond to JH after commitment (Riddiford, 1980). Hence, in the present study, we speculate that the imaginal cells require JH for pupal differentiation and it is likely that the disruption of JH action in the imaginal tissues, as a consequence of TcMet RNAi, results in adult overshoot. In contrast, the abdominal epidermis remains pupal, as differences in action of JH do not influence the pupal programming, once committed. Also, it is interesting to note that, irrespective of variation in the commitment period among insects, the role of JH in promoting the pupal differentiation of the imaginal tissues at the end of the larval stage appears to be conserved.

How does JH prevent precocious adult development in pupally committed tissues? The pupal specifying gene, Broad, is one of the early ecdysone response genes whose expression activates the tissue specific late ecdysone response genes during the prepupal development (Karim et al. 1993; Bayer et al. 1997; Zhou et al. 1998). JH can prevent initial onset of 20E-induced Broad expression (Zhou et al. 1998; Zhou and Riddiford, 2002). Also, Broad levels must decline before adult commitment during the pupal stage and application of ectopic JH to pupal stage induced second pupal cuticle instead of adult cuticle in *M. sexta* and abdominal epidermis of *D. melanogaster* (Zhou and Riddiford, 2002). Hence, under normal conditions, decline in JH titers at the time of commitment peak of 20E during the final instar allows 20E-induced Broad expression resulting in pupal commitment. JH levels rise again at the end of the larval stage and JH appears to maintain Broad expression in pupally committed imaginal tissues, preventing precocious adult cuticle deposition. Disruption of Broad expression in the final instar leads to larval-pupal-adult intermediate forms and improper development of imaginal structures such as wings (Uhlivora et al. 2003; Parthasarathy et al. 2008; Suzuki et al. 2008; Konopova and Jindra, 2008). However, the severity of adult overshoot observed with TcMet RNAi phenotypes was not observed with the Broad RNAi insects, possibly due to failure to block JH action in Broad RNAi insects (Suzuki et al. 2008). Recently, Konopova and Jindra (2008) showed that TcMet acts upstream of Broad and regulates its expression differentially in the larval and pupal stages. However, TcMet RNAi insects eventually showed precocious development of adult structures in the imaginal tissues at 176 h after injection, well beyond the quiescent stage. In correlation with the previous studies, it is likely that JH action in maintaining Broad expression in the imaginal tissues to prevent precocious adult development is disrupted by knock-down of TcMet during the quiescent stage.

Effect of Met RNAi on remodeling of internal tissue

Because TcMet RNAi disrupted larval-pupal ecdysis but allowed pupal development beneath the larval skin, we investigated the effect of TcMet RNAi on the remodeling of internal tissue, midgut. The midgut undergoes remodeling during larval-pupal metamorphosis in *T. castaneum* (Parthasarathy and Palli, 2008). The larval cells degenerate by PCD and ISCs proliferate and differentiate into pupal gut epithelium. Some of the ISCs in the pupal gut epithelium proliferate after pupation and evaginate as crypts (a characteristic feature of adult midgut) during the end of the pupal stage. Interestingly, depletion of TcMet RNA levels did

NIH-PA Author Manuscript

NIH-PA Author Manuscript

NIH-PA Author Manuscript

not completely block midgut remodeling. The elimination of larval gut through PCD was on par with the control; however, the differentiation of pupal midgut from larval ISCs and evagination of crypts in the anterior region of midguts in TcMet RNAi insects were delayed when compared to those in control insects. The evagination of crypts in the posterior region of midguts in TcMet RNAi insects was observed, though the size of the crypts was much smaller than in midguts dissected from control larvae. As midgut remodeling events proceed from posterior to anterior ends in insects (Nishiura and Smouse, 2000; Wu et al. 2006), the delay in the differentiation of pupal midgut and evagination of crypts was obvious in TcMet RNAi insects due to the developmental arrest rather than the direct effect of TcMet mRNA deficiency. However, the role of TcMet in midgut remodeling could not be completely ruled out, as we do see TcMet mRNA expression in the midgut tissue during larval-pupal metamorphosis. Also, Pursley et al (2000) showed that Met protein localization in the imaginal tissues of *D. melanogaster* including the midgut imaginal cells (stem cells) during larval-pupal metamorphosis. Surprisingly, silencing of TcMet in midgut did not disrupt the JH action as revealed by our *in vitro* cell proliferation assay. JH suppression of 20E-induced cell proliferation was not affected in the TcMet RNAi insects. This might be due to two reasons: either TcMet does not play a major role in midgut tissue as speculated above or the level of suppression of TcMet mRNA levels in midgut (50% levels when compared to control at two days after injection followed by one or two days of *in vitro* culturing, data not shown) is not sufficient to block JH action in the midgut. Based on the external morphology and internal tissue remodeling of TcMet RNAi insects, it is clear that silencing of Met does not block the preparation of insects to pupal programming but determines the final fate to some JH dependent tissues such as imaginal structures.

T. castaneum, because of its high sensitivity to JH, presence of a single ortholog of Met and gce, and efficient function of RNAi, offers an excellent model system to study JH action (Willis, 2007). This paper provides new insights into the function of TcMet in mediating JH action at the end of the final instar in promoting larval-pupal transition by preventing precocious adult development. Further investigations on targets of TcMet in JH signaling pathway, which are underway in our laboratory, should reveal the mechanism of Met action in JH signal transduction.

4. Methods

4.1. Rearing and staging

T. castaneum (Haliscak and Beeman, 1983) Strain GA-1 beetles were reared on organic wheat flour containing 10% yeast at 30°C under standard conditions (Beeman and Stuat, 1990). Precise staging was done from the final instar to adults according to Parthasarathy et al. (2007). Briefly, the final instar lasts for 6 days (144 h AEFI, after ecdysis into final instar): 72 h of feeding stage, 24 h of non-feeding wandering stage, followed by 48 h of non-feeding quiescent stage (prepupa). The pupal stage lasts for 4 days (96 h).

4.2. Hydroprene treatment

Hydroprene (Ethyl (2E,4E,7S)-3,7,11-trimethyl-2,4-dodecadienoate) was a gift from Wellmark International (Dallas, TX). Technical grade compound was dissolved in acetone and used at a final concentration of 1 ppm in feeding bioassays at 24 h AEFI. For topical application, 0.5 μl of Hydroprene (2 μg/ml) in acetone was applied on the dorsal side of thorax and abdomen at 96 h AEFI. All control larvae were treated with equivalent amounts of acetone alone.

4.3. Double-stranded RNA (dsRNA) synthesis and injection

TcMet dsRNA was synthesized using the Ambion MEGAscript transcription kit (Ambion, Austin, TX). Cognate primers, (forward primer, 5'- TAAGGCGGCAAACTC-3' and reverse

NIH-PA Author Manuscript

NIH-PA Author Manuscript

NIH-PA Author Manuscript

primer, 5'-TGGCTCAACCGACTCGTC-3') designed based on the sequence available in the GenBank (Glean_16205, Accession number XP_966542), containing T7 polymerase promoter sequence at their 5' ends were used to amplify regions of TcMet. The resultant PCR product (300 bp) was used for transcription reaction as per the instruction manual. dsRNA was injected into the larvae on the dorsal side of the first or second abdominal segments using a aspirator tube assembly (Sigma) fitted with 3.5" glass capillary tube (Drummond) pulled by a needle puller (Model P-2000, Sutter Instruments Co.). Injected larvae were reared under standard conditions until use. Control larvae were injected with dsRNA prepared using *E. coli malE* gene fragment as a template.

4.4. cDNA synthesis and Quantitative real-time reverse-transcriptase PCR (qRT-PCR)

Total RNA was extracted from whole body or midguts dissected from staged larvae and pupae using TRI reagent (Molecular Research Center Inc., Cincinnati, OH). cDNA was synthesized using 2 μg of DNAse1 (Ambion, Austin, TX) – treated RNA and iScript cDNA synthesis kit (Biorad Laboratories, Hercules, CA) in a 20 μl reaction volume as per the manufacturer's instructions. Real-time quantitative reverse-transcriptase PCR was performed using MyiQ single color real-time PCR detection system (Biorad Laboratories). PCR reaction components were:1 μl of cDNA, 1 μl each of forward and reverse sequence specific primers (TcMet, forward primer 5' GGGAAAGCAAAGGATCATCA 3' and reverse prime 5' AAGGCCTTCTTGCTCACTCA 3', the sequences of other primers have been reported by Parthasarathy et al. 2008), 7 μl of H_2O and 10 μl of supermix (Biorad Laboratories). PCR conditions were: 95°C for 3 min followed by 45 cycles of 95°C for 10seconds, 60°C for 20 seconds, 72°C for 30 seconds. Both the PCR efficiency and R^2 (correlation coefficient) values were taken into account prior to estimating the relative quantities. Relative expression levels of each gene were quantified using ribosomal protein (rp49) expression levels as an internal control.

4.5. Preparation of tissue sections, BrdU and TUNEL assays

Staged larvae/pupae were injected with 0.1 μl of 10 mM BrdU (Roche, Indianapolis, IN) into the haemocoel as described above. After 12 h, the midguts from injected insects were dissected. The tissues were processed using 5-Bromo-2'-deoxy-uridine Labeling and Detection kit I (Roche) according to manufacturer's instructions. The tissues were incubated with Texas-Red conjugated goat anti-mouse antibody (Molecular Probes) at 1:1000 dilutions. Controls included were midguts from insects that were not injected and midguts that were not exposed to anti-BrdU. After washing extensively in 1XPBS, the tissues were counterstained with DAPI and mounted with 50% glycerol in 1X PBS.

For preparation of tissue sections, the midguts from larvae and pupae injected with dsRNA for specific genes were dissected in 1XPBS (phosphate buffered saline, Sigma) and fixed in 4% paraformaldehyde (Sigma). Sectioning was done as previously described (Parthasarathy and Palli, 2007). The sections were deparaffinized through successive baths of Xylene, rehydrated through serial grades of ethanol, water and 1XPBS. The sections were processed for BrdU assay as described above or for TUNEL assay (Parthasarathy and Palli, 2008). The nuclear counter-staining was done with DAPI (4', 6-Diamidino-2-phenyl indole, Sigma) at 1 μg/ml concentration for 10 min. The slides were washed with 1XPBS twice and mounted in 50% glycerol.

4.6. In vitro assays

The abdominal tissues dissected from insects injected with dsRNA were cultured in Ex-Cell 420 Insect serum free medium (JRH Biosciences) containing the following antibiotics: antibiotic - antimycotic solution, 1X dilution (Sigma); Gentamicin solution, 200 μg/ml (Sigma); Penicillin-Streptomycin, 20 units/ml (Life Technologies) for 24 h at 27°C. The entire

NIH-PA Author Manuscript

NIH-PA Author Manuscript

NIH-PA Author Manuscript

medium was replaced with medium containing DMSO or 10 μM of JH III and exposed for 6 h. The tissues were used for qRT-PCR analysis.

The midguts dissected under aseptic conditions were cultured as mentioned above. The entire medium was replaced with fresh medium containing appropriate concentrations of ligands (10 μM of 20E, JH III or both Sigma) and incubated for further 24 h. The tissues were used for BrdU assay. For BrdU incorporation, the midguts were pulsed with BrdU labeling reagent (Roche) at 1:1000 dilutions (final concentration 10 μM) for 12 h during this 24 h incubation period. The midguts were washed with 1XPBS and fixed in 4% paraformaldehyde for 1 h at room temperature. The tissues were processed for BrdU as described above.

4.7. Imaging and documentation

For light microscopy, the modular zoom system (Leica Z16 APO, Germany) fitted with JVC 3CCD Digital Camera KY-F75U was used. The images were documented using Cartograph version 6.1.0 (GT Vision Demonstration). Image processing was done using Archimed version 5.2.2 (Micovision Instruments).

For scanning electron microscopy, the insects were washed thoroughly in double distilled water thrice and then briefly in 0.1 % Triton X-100 detergent solution to get rid of flour adhering to the insect. The insects were processed according to Nation (1983). Briefly, the insects were slowly dehydrated in series of ethanol (25, 50, 75, 90 and 100%) by incubating in each concentration for 1 h with shaking. The insects were then immersed in HDMS (1,1,1,3,3,,3 hexadimethyldisilazane) for 5 min., and air dried at room temperature. The insects were mounted on stainless steel stubs with sticky tape (RPI) under dust free conditions. The insects were then sputtered with gold using Hummer VI Sputtering System (Technics) at plasma discharge rate of 10 milliamperes for 180 s. Scans were performed with a Hitachi S-800 Scanning Electron Microscope at 10 kV and 10 milliamperes. Images were documented using Evex Nanoanalysis and Digital Imaging software (Evex Analytical version 2.0.1192).

For fluorescent images, an Olympus FV1000 laser scanning confocal microscope was used. DAPI, GFP, and RFP were excited using 405 nm, 485 nm, and 543 nm laser lines, respectively. When using multiple fluors simultaneously, images were acquired sequentially, line-by-line, in order to reduce excitation and emission cross talk. The primary objective used was an Olympus water immersion PLAPO40XWLSM-NA1.0. Image acquisition was conducted at a resolution of 512×512 pixels and a scan-rate of 10 ms/pixel. Control of the microscope, as well as image acquisition and exportation as TIFF files, was conducted using Olympus Fluoview software version 1.5. Exposure settings that minimized oversaturated pixels in the final images were used. Optical sectioning was done and a composite Z-stack image was used, wherever necessary. Figures of all micrographs were assembled using Photoshop 7.0.

Acknowledgements

This work was supported by National Science Foundation (IBN-0421856) and National Institutes of Health (RO1 GM070559-03). We thank Drs. Michael Goodin, Sheryn Perry, and Michael Sharkey and Mr. Dicky Yu for their help in histology and microscopic facilities. This is contribution number 08-08-75 from the Kentucky Agricultural Experimental Station.

References

Arakane Y, Muthukrishnan S, Kramer KJ, Specht CA, Tomoyasu Y, Lorenzen MD, Kanost M, Beeman RW. The *Tribolium* chitin synthase genes TcCHS1 and TcCHS2 are specialized for synthesis of epidermal cuticle and midgut peritrophic matrix. Insect Mol. Biol 2005;14:453–463. [PubMed: 16164601]

Ashburner M. Effects of juvenile hormone on adult differentiation of *Drosophila melanogaster*. Nature 1970;227:187–189. [PubMed: 5428413]

NIH-PA Author Manuscript

NIH-PA Author Manuscript

NIH-PA Author Manuscript

Ashok M, Turner C, Wilson TG. Insect juvenile hormone resistance gene homology with the bHLH-PAS family of transcriptional regulators. Proc. Natl. Acad. Sci. U S A 1998;95:2761–2766. [PubMed: 9501163]

Baker FC, Tsai LW, Reuter CC, Schooley DA. *In vivo* fluctuation of JH, JH acid, and ecdysteroid titer, and JH esterase activity during development of the fifth stadium *Manduca sexta*. Insect Biochem 1987;17:989–996.

Bayer CA, von Kalm L, Fristrom JW. Relationships between protein isoforms and genetic functions demonstrate functional redundancy at the Broad-Complex during *Drosophila* metamorphosis. Dev. Biol 1997;187:267–282. [PubMed: 9242423]

Beeman RW, Staurt JJ. A gene for lindane+cyclodeine resistance in the red flour beetle (Coleoptera: Tenebrionidae). J. Econ. Entomol 1990;83:1745–1751.

Bounhiol JJ. Recherches experimentales sur le determinisme de la metamorphose chez les Lepidopteres. Biol. Bull. Suppl 1938;24:1–199.

Connat JL, Delbecque JP, Delachambre J. The onset of metamorphosis in *Tenebrio molitor*: effects of a juvenile hormone analogue and of 20-hydroxyecdysone. J. Insect Physiol 1984;30:413–419.

Flatt T, Kawecki TJ. Pleiotropic effects of methoprene-tolerant (Met), a gene involved in juvenile hormone metabolism, on life history traits in *Drosophila melanogaster*. Genetica 2004;122:141–160. [PubMed: 15609573]

Godlewski J, Wang S, Wilson TG. Interaction of bHLH-PAS proteins involved in juvenile hormone reception in *Drosophila*. Biochem. Biophys. Res. Commun 2006;342:1305–1311. [PubMed: 16516852]

Haliscak JP, Beeman RW. Status of malathion resistance in five genera of beetles infesting farm-stored corn, wheat and oats in the United States. J. Econ. Entomol 1983;76:717–722.

Hiruma K. Possible roles of juvenile hormone in the prepupal stage of *Mamestra brassicae*. Gen. Comp. Endocrinol 1980;41:392–399. [PubMed: 7409447]

Hiruma K, Shinoda T, Malone F, Riddiford LM. Juvenile hormone modulates 20-hydroxyecdysone-inducible ecdysone receptor and ultraspiracle gene expression in the tobacco hornworm, *Manduca sexta*. Dev. Genes Evol 1999;209:18–30. [PubMed: 9914415]

Karim FD, Guild GM, Thummel CS. The *Drosophila* Broad Complex plays a key role in controlling ecdysone-regulated gene expression at the onset of metamorphosis. Development 1993;118:977–988. [PubMed: 8076529]

Kethidi DR, Perera SC, Zheng S, Feng QL, Krell P, Retnakaran A, Palli SR. Identification and characterization of a juvenile hormone (JH) response region in the JH esterase gene from the spruce budworm, *Choristoneura fumiferana*. J. Biol. Chem 2004;279:19634–19642. [PubMed: 14990570]

Kiguchi K, Riddiford LM. The role of juvenile hormone in pupal development of the tobacco hornworm, *Manduca sexta*. J. Insect Physiol 1978;24:673–680.

Konopova B, Jindra M. Juvenile hormone resistance gene Methoprene-tolerant controls entry into metamorphosis in the beetle *Tribolium castaneum*. Proc. Natl. Acad. Sci. USA 2007;104:10488–10493. [PubMed: 17537916]

Konopova B, Jindra M. Broad-complex acts downstream of Met in JH signaling to coordinate primitive holometabolan metamorphosis. Development 2008;135:559–568. [PubMed: 18171683]

Kostyukovsky M, Chen B, Atsmi S, Shaaya E. Biological activity of two juvenoids and two ecdysteroids against three stored product insects. Insect Biochem. Mol. Biol 2000;30:891–897. [PubMed: 10876135]

Koyama T, Obara Y, Iwami M, Sakarai S. Commencement of pupal commitment in late penultimate instar and its hormonal control in wing imaginal discs of silkworm, *Bombyx mori*. J. Insect Physiol 1994;50:123–133. [PubMed: 15019513]

Kurushima M, Ohtaki T. Relation between cell number and pupal development of wing discs in *Bombyx mori*. J. Insect Physiol 1975;21:1705–1712.

Minakuchi C, Zhou X, Riddiford LM. Kruppel homolog 1 (Kr-h1) mediates juvenile hormone action during metamorphosis of *Drosophila melanogaster*. Mech. Dev 2008;125:91–105. [PubMed: 18036785]

Moore AW, Barbel S, Jan LY, Jan YN. A genome wide survey of basic helix-loop-helix factors in *Drosophila*. Proc. Natl. Acad. Sci. U.S.A 2000;97:10436–10441. [PubMed: 10973473]

NIH-PA Author Manuscript

NIH-PA Author Manuscript

NIH-PA Author Manuscript

Muramatsu D, Kinjoh T, Shinoda T, Hiruma K. The role of 20-hydroxyecdysone and juvenile hormone in pupal commitment of the epidermis of the silkworm, *Bombyx mori*. Mech. Dev. 2008

Nation JL. A new method using hexamethyldisilazane for preparation of soft insect tissues for scanning electron microscopy. Stain Tech 1983;58:347–351.

Nijhout HF. Dynamics of juvenile hormone action in larvae of the tobacco hornworm, *Manduca sexta*. Biol. Bull 1975;149:568–579. [PubMed: 1203337]

Nijhout HF, Wheeler DE. Juvenile hormone and the physiological basis of insect polymorphism. Quarterly Review of Biology 1982;57:109–133.

Nishiura JT, Smouse D. Nuclear and cytoplasmic changes in the *Culex pipens* (Diptera: Culicidae) alimentary canal during metamorphosis and their relationship to programmed cell death. Ann. Entomol. Soc. Am 2000;93:282–290.

Parthasarathy R, Palli SR. Developmental and hormonal regulation of midgut remodeling in a lepidopteran insect, *Heliothis virescens*. Mech Dev 2007;124:23–34. [PubMed: 17107775]

Parthasarathy R, Tan A, Bai H, Palli SR. Transcription factor broad suppresses precocious development of adult structures during larval-pupal metamorphosis in the red flour beetle, *Tribolium castaneum*. Mech Dev 2008;125:299–313. [PubMed: 18083350]

Parthasarathy R, Palli SR. Proliferation and differentiation of intestinal stem cells during metamorphosis of the red flour beetle, *Tribolium castaneum*. Dev. Dyn. 2008

Piepho H. Versuche uber die Rolle von Wirkstoffen in der Metamorphose der Schmetterlinge. Biol. Zbl 1945;65:141–148.

Postlethwait JH. Juvenile hormone and the adult development of *Drosophila*. Biol. Bull 1974:147.

Pursley S, Ashok M, Wilson TG. Intracellular localization and tissue specificity of the Methoprene-tolerant (Met) gene product in *Drosophila melanogaster*. Insect Biochem. Mol. Biol 2000;30:839–845. [PubMed: 10876128]

Quennedey A, Quennedey B. Development of the wing discs of *Zophobas atratus* under natural and experimental conditions: occurrence of a gradual larval-pupal commitment in the epidermis of tenebrionid beetles. Cell Tissue Res 1999;296:619–634. [PubMed: 10370149]

Restifo LL, Wilson TG. A juvenile hormone agonist reveals distinct developmental pathways mediated by ecdysone-inducible broad complex transcription factors. Dev. Genet 1998;22:141–159. [PubMed: 9581286]

Riddiford LM. Ecdysone-induced change in cellular commitment of the epidermis of the tobacoo hornworm, *Manduca sexta* at the initiation of metamorphosis. Gen. Comp. Endocrinol 1978;34:438–446. [PubMed: 648872]

Riddiford LM. Insect endocrinology: action of hormones at the cellular level. Annu. Rev. Physiol 1980;42:511–528. [PubMed: 6996595]

Riddiford LM. Hormone action at the cellular level. Comprehensive Insect Physiology, Biochemistry and Pharmocology 1985;7:37–84.

Riddiford, LM. Hormones and Drosophila development. In: Bate, M.; Martinez, AM., editors. The development of *Drosophila melanogaster*. Vol. II. New York: Cold Spring Harbor Laboratory press; 1993. p. 899-939.

Riddiford LM. Cellular and molecular actions of juvenile hormone. I. General considerations and premetamorphic actions. Adv. Insect Physiol 1994;24:213–274.

Riddiford LM, Ashburner M. Effects of juvenile hormone mimics on larval development and metamorphosis of *Drosophila melanogaster*. Gen. Comp. Endocrinol 1991;82:172–183. [PubMed: 1906823]

Riddiford LM, Baeckmann A, Hice RH, Rebers J. Developmental expression of three genes for larval cuticular proteins of the tobacco hornworm, *Manduca sexta*. Dev. Biol 1986;118:82–94. [PubMed: 3770309]

Riddiford LM, Hiruma K, Zhou X, Nelson CA. Insights into the molecular basis of the hormonal control of molting and metamorphosis from *Manduca sexta* and *Drosophila melanogaster*. Insect Biochem. Mol. Biol 2003;33:1327–1338. [PubMed: 14599504]

Suzuki Y, Truman JW, Riddiford LM. The role of Broad in the development of *Tribolium castaneum*. Implications for the evolution of the holometabolous insect pupa. Dev 2008;135:569–577.

NIH-PA Author Manuscript

NIH-PA Author Manuscript

NIH-PA Author Manuscript

Tan A, Palli SR. Identification and characterization of nuclear receptors from the red flour beetle, *Tribolium castanuem*. Insect Biochem. Mol. Biol. 2007In Press

Truman JW, Riddiford LM. The origins of insect metamorphosis. Nature 1999;410:447–452. [PubMed: 10519548]

Truman JW, Riddiford LM. Endocrine insights into the evolution of metamorphosis in insects. Annu. Rev. Entomol 2002;47:467–500. [PubMed: 11729082]

Truman JW, Riddiford LM, Safranek L. Temporal patterns of response to ecdysone and juvenile hormone in the epidermis of the tobacco hornworm, *Manduca sexta*. Dev. Biol 1974;39:247–262. [PubMed: 4854621]

Uhlirova M, Foy BD, Beaty BJ, Olson KE, Riddiford LM, Jindra M. Use of Sindbis virus-mediated RNA interference to demonstrate a conserved role of Broad-Complex in insect metamorphosis. Proc. Natl. Acad. Sci. U. S. A 2003;100:15607–15612. [PubMed: 14668449]

Wang S, Baumann A, Wilson TG. *Drosophila melanogaster* Methoprene-tolerant (Met) gene homologs from three mosquito species: Members of PAS transcriptional factor family. J. Insect Physiol 2007;53:246–253. [PubMed: 17166512]

Williams CM. The juvenile hormone.I. Its role in the endocrine control of molting, pupation, and adult development of the cecropia silkworm. Biol. Bull 1961;121:572–585.

Willis JH. Metamorphosis starts with Met. Proc. Natl. Acad. Sci. U S A 2007;104:10297–10298. [PubMed: 17566102]

Wilson TG. Genetic evidence that mutants of the methoprene-tolerant gene of *Drosophila melanogaster* are null mutants. Arch. Insect Biochem. Physiol 1996;32:641–649. [PubMed: 8756311]

Wilson TG, Ashok M. Insecticide resistance resulting from an absence of target-site gene product. Proc. Natl. Acad. Sci. U S A 1998;95:14040–14044. [PubMed: 9826649]

Wilson TG, Fabian J. A *Drosophila melanogaster* mutant resistant to a chemical analog of juvenile hormone. Dev. Biol 1986;118:190–201. [PubMed: 3095161]

Wilson TG, Wang S, Beno M, Farkas R. Wide mutational spectrum of a gene involved in hormone action and insecticide resistance in *Drosophila melanogaster*. Mol. Genet. Genomics 2006a;276:294–303. [PubMed: 16802158]

Wilson TG, Yerushalmi Y, Donnell DM, Restifo LL. Interaction Between Hormonal Signaling Pathways in *Drosophila melanogaster* as Revealed by Genetic Interaction Between Methoprene-tolerant and Broad-Complex. Genetics 2006b;172:253–264. [PubMed: 16204218]

Wu Y, Parthasarathy R, Bai H, Palli SR. Mechanisms of midgut remodeling: juvenile hormone analog methoprene blocks midgut metamorphosis by modulating ecdysone action. Mech. Dev 2006;123:530–547. [PubMed: 16829058]

Zhou B, Hiruma K, Shinoda T, Riddiford LM. Juvenile hormone prevents ecdysteroid-induced expression of broad complex RNAs in the epidermis of the tobacco hornworm, *Manduca sexta*. Dev. Biol 1998;203:233–244. [PubMed: 9808776]

Zhou X, Riddiford LM. Broad specifies pupal development and mediates the 'status quo' action of juvenile hormone on the pupal-adult transformation in *Drosophila* and *Manduca*. Development 2002;129:2259–2269. [PubMed: 11959833]

NIH-PA Author Manuscript
NIH-PA Author Manuscript
NIH-PA Author Manuscript

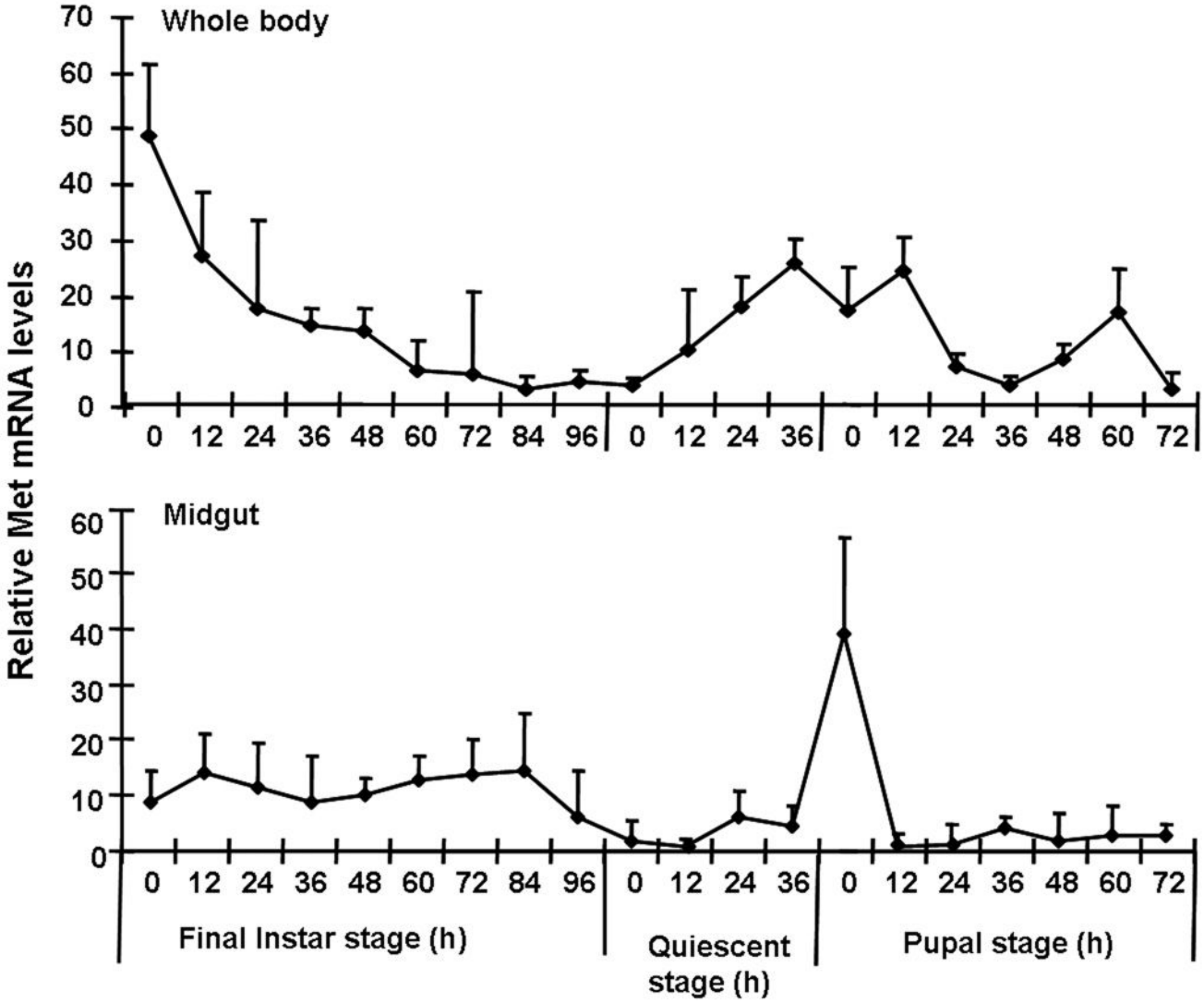

Fig. 1.

mRNA levels of TcMet in the whole body and the midgut of *T. castaneum* determined by quantitative reverse-transcriptase real-time PCR (qRT-PCR). Samples were collected at 12 h interval during the final instar and pupal stages. Total RNA was extracted from pools of three larvae for each treatment. The Y-axis denotes expression levels normalized using the rp49 levels as an internal control. Mean ± S.E. of two independent experiments with three replications each are shown.

NIH-PA Author Manuscript

NIH-PA Author Manuscript

NIH-PA Author Manuscript

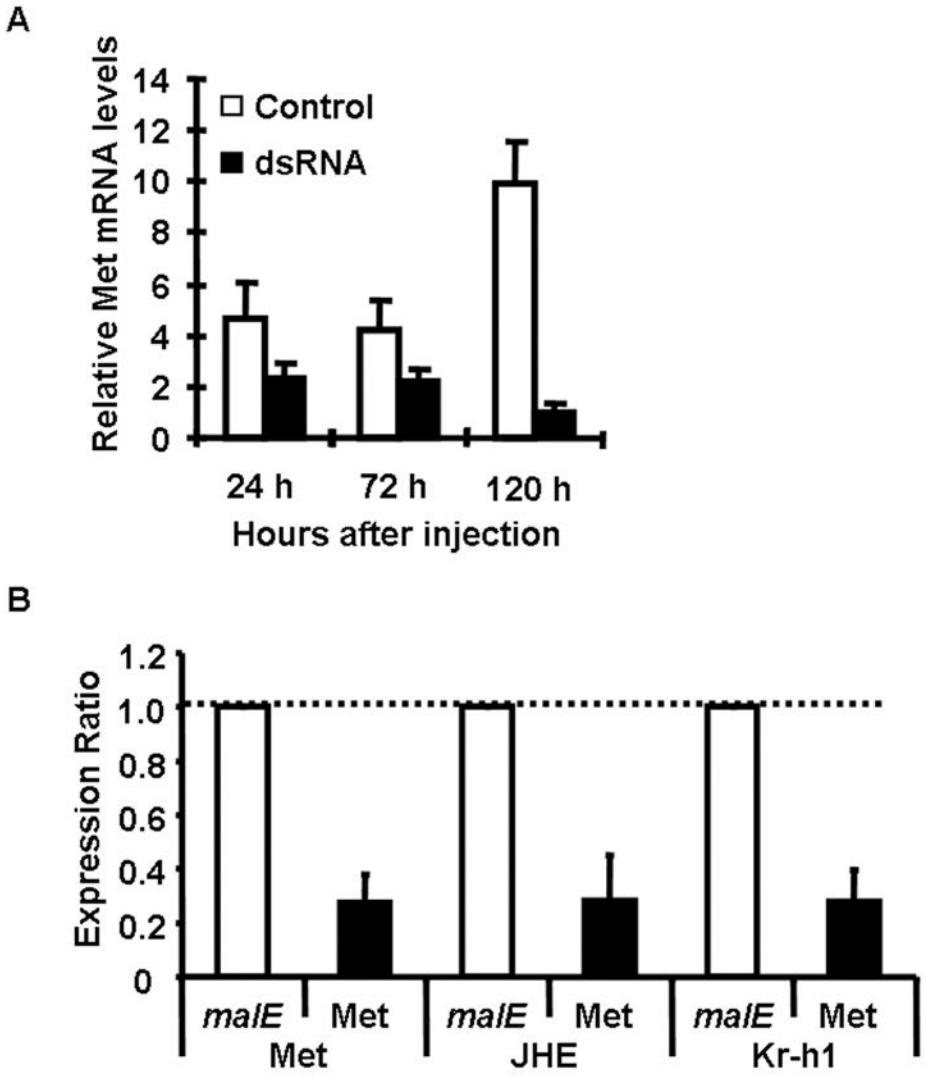

NIH-PA Author Manuscript
NIH-PA Author Manuscript
NIH-PA Author Manuscript

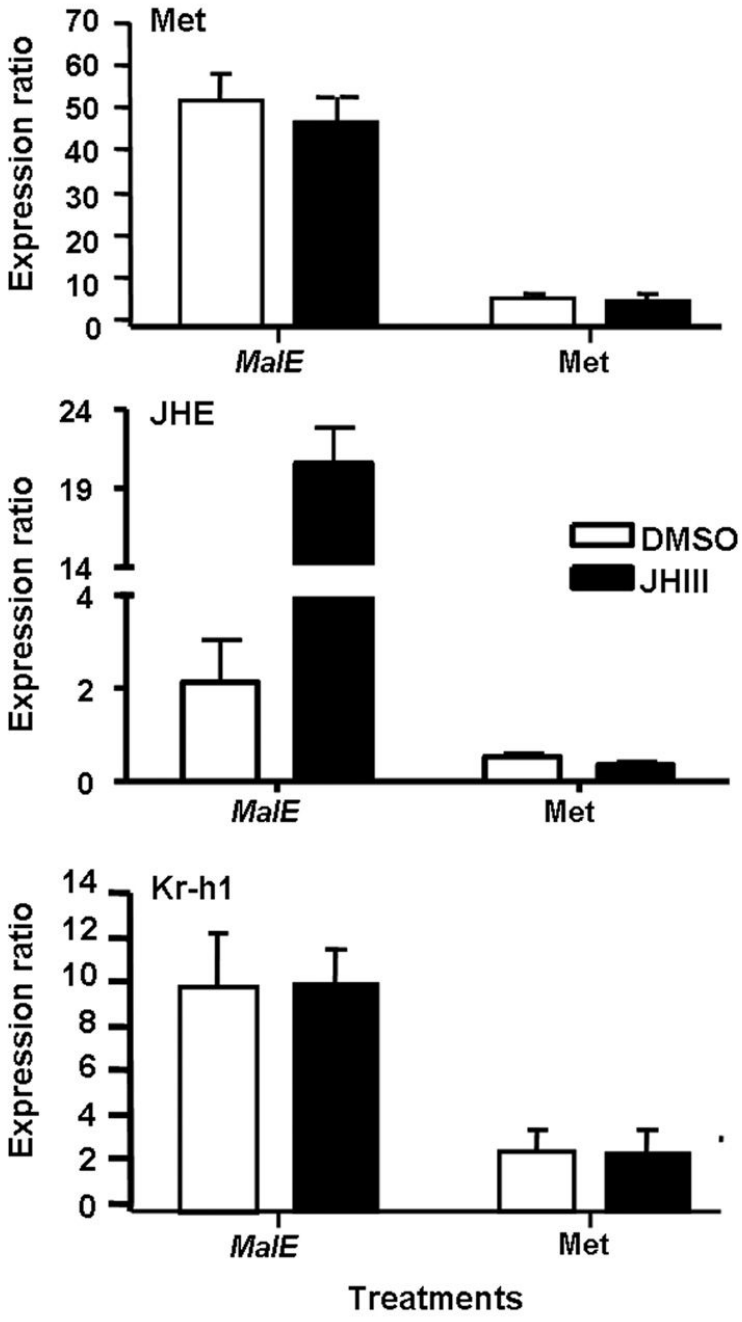

Fig. 2.

A) mRNA levels of TcMet in dsRNA injected and control insects. dsRNA injections were done at 24 AEFI. The insects were sampled at 24, 72 and 120 h after injection. Total RNA was extracted from three larvae for each treatment. cDNAs prepared from the RNA were used in qRT-PCR. The relative expression levels of TcMet mRNA were determined using the levels of rp49 as an internal control. Mean ± S.E. of three independent experiments are shown.

B) The expression ratio of mRNA levels of Met, JHE and Kr-h1 in insects injected with TcMet dsRNA using qRT-PCR. Injections were given at 24 h AEFI. Total RNA was extracted from pools of three larvae for each treatment at three days after injection. The mRNA levels were normalized using the levels of rp49 as an internal control. The expression levels of each gene

NIH-PA Author Manuscript

NIH-PA Author Manuscript

NIH-PA Author Manuscript

in the corresponding control insects injected with *malE* dsRNA was set as 1. Mean ± S.E. for three biological replicates are shown.

C) Ratio of mRNA levels of genes in cultured abdominal tissues from TcMet and *malE* dsRNA injected insects. Abdominal tissues including epidermis, fat body, midgut etc. (dissected from larvae at 96 h AEFI that were injected with dsRNA at 24 h AEFI) were cultured *in vitro* in the medium containing DMSO or 10 μM JH III. RNA was extracted and mRNA levels were quantified using qRT-PCR. Mean ± S.E of three replicates for each treatment are shown.

NIH-PA Author Manuscript
NIH-PA Author Manuscript
NIH-PA Author Manuscript

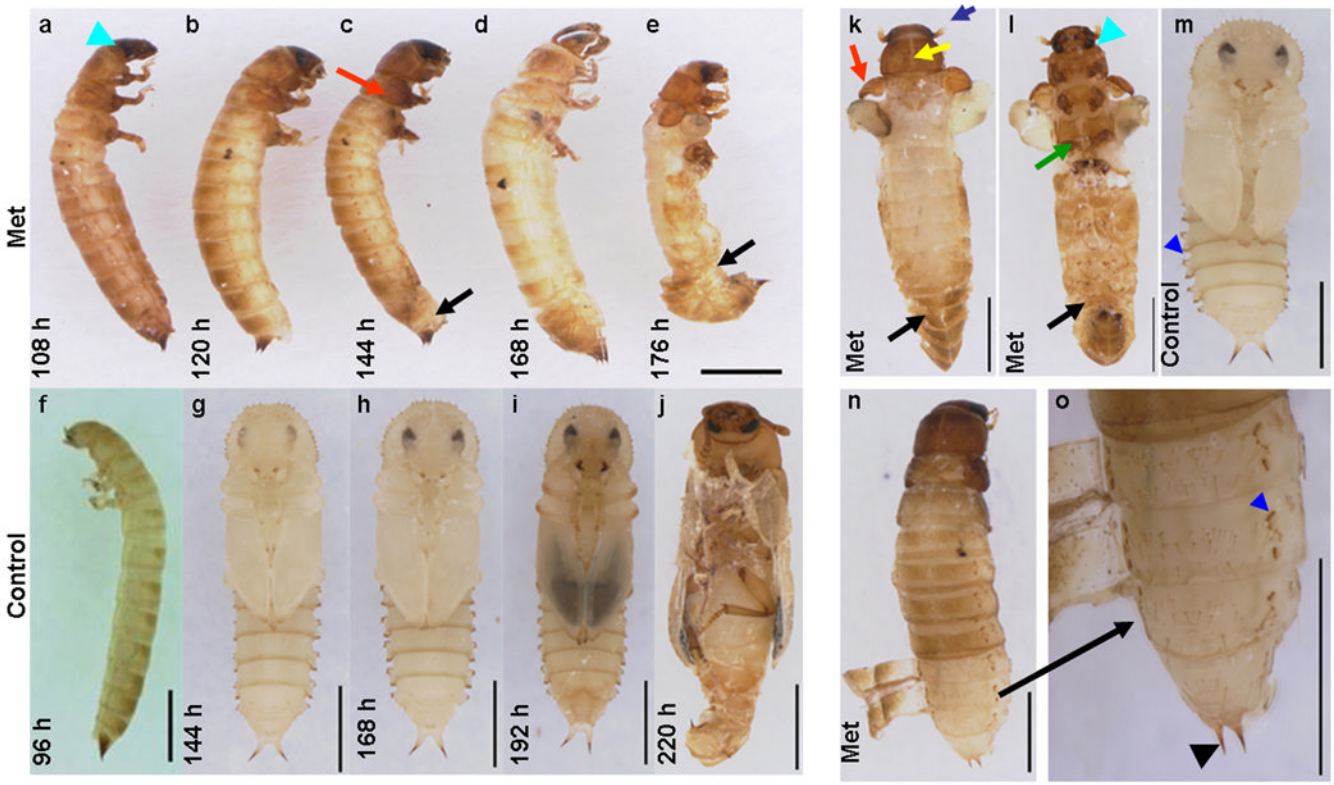

NIH-PA Author Manuscript
NIH-PA Author Manuscript
NIH-PA Author Manuscript

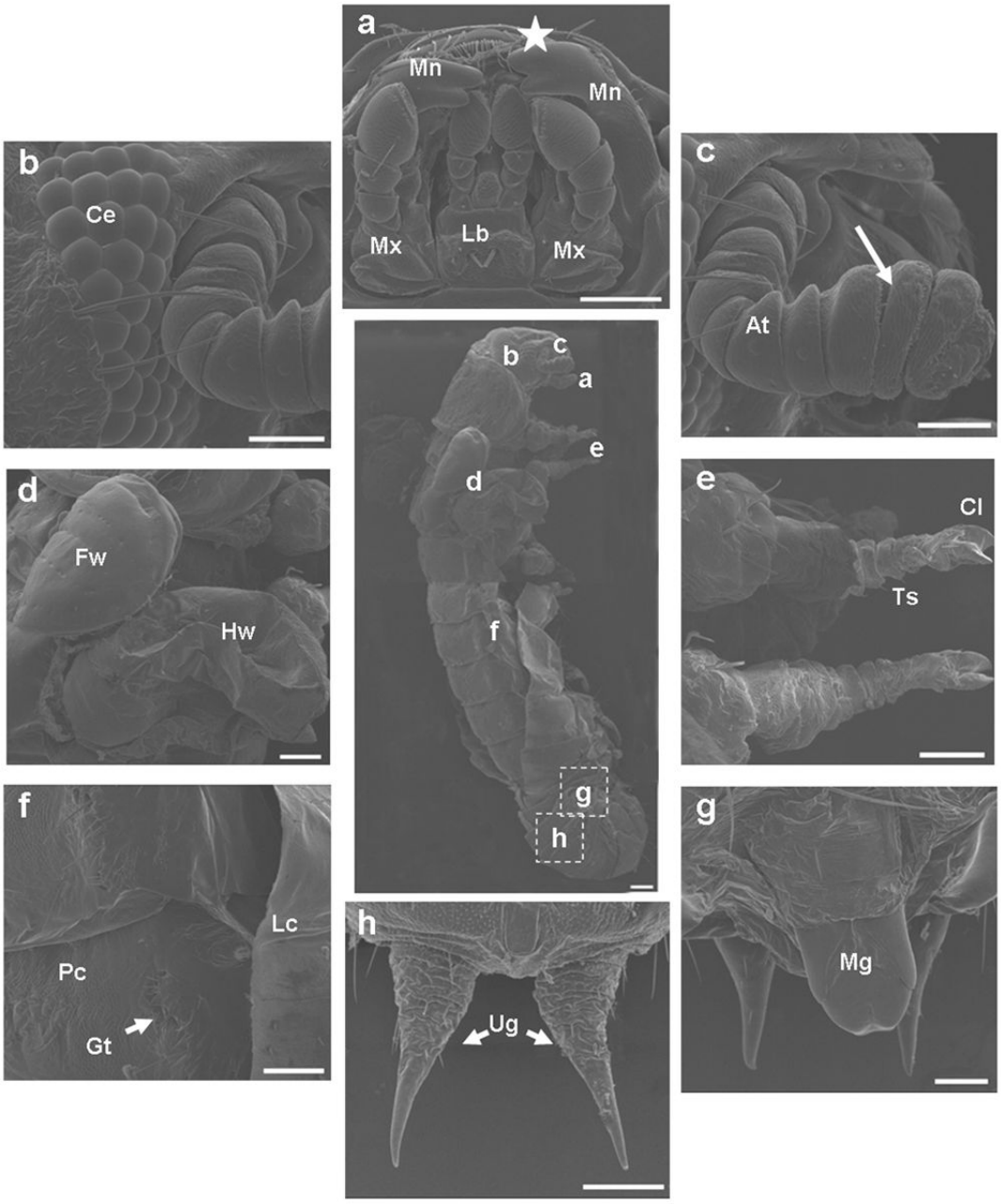

NIH-PA Author Manuscript
NIH-PA Author Manuscript
NIH-PA Author Manuscript

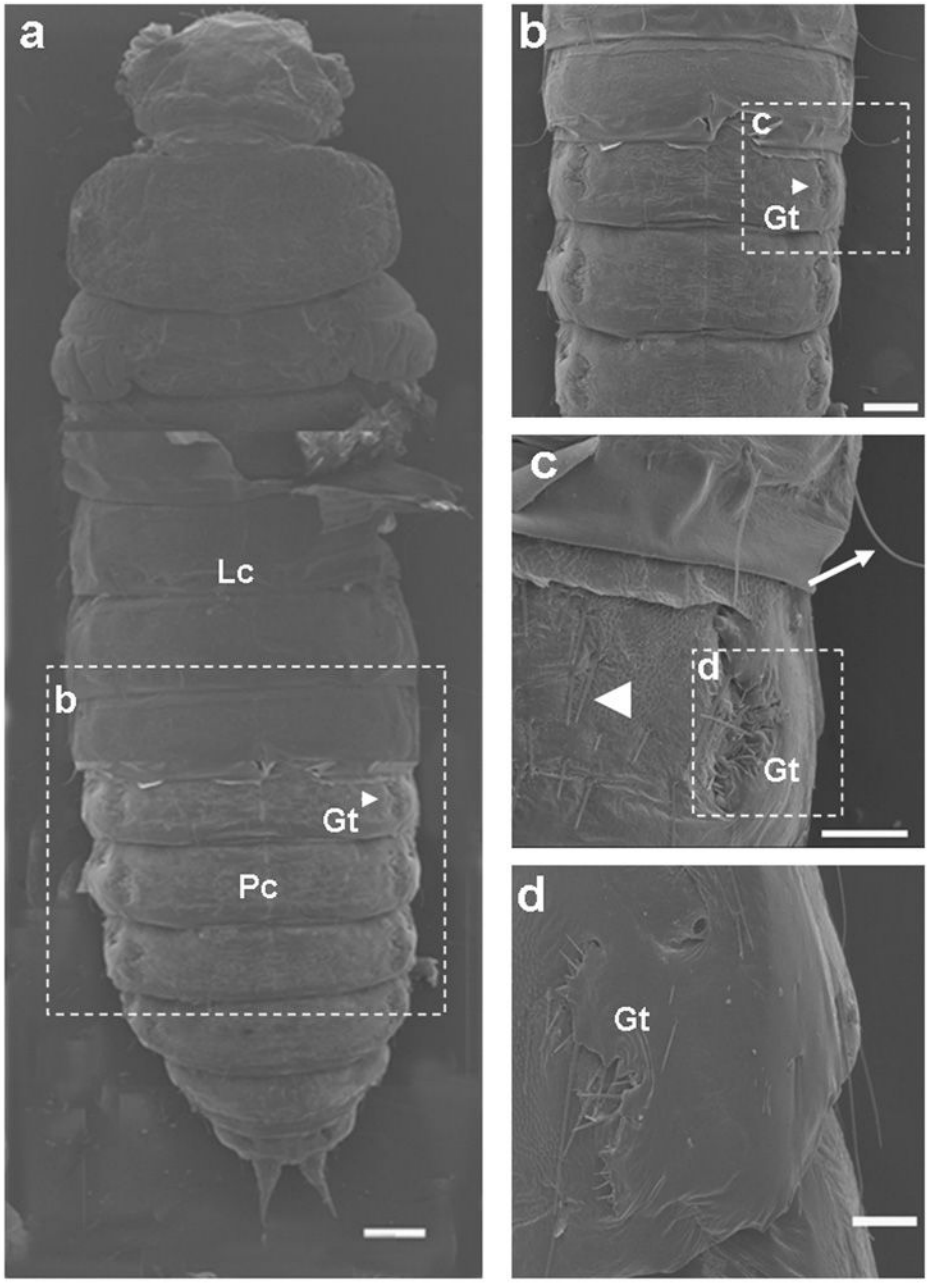

Fig. 3.

A. Phenotypes of knock-down of TcMet. TcMet or *malE* dsRNA (control) was injected at 24 h AEFI and the corresponding phenotypes are shown in comparison with control taken using a light microscope (a–o). Panels a–e show lateral view of insects injected with TcMet dsRNA. Note the development of compound eyes (a, blue arrowhead), sclerotization of head and thoracic region (b), sclerotization of wing pads (c, red arrow) beneath the larval skin, initiation of ecdysis (c, black arrow), continuation of ecdysis (d) and incomplete ecdysis with larval exuvium attached to abdomen (e, black arrow). Panels f–j show insects injected with *malE* dsRNA (control); panel f- lateral view of the quiescent stage, panels g–j – ventral view of pupal stages. Time points in panels a–j indicate hours after injection. Note the delay in larval-pupal

NIH-PA Author Manuscript

NIH-PA Author Manuscript

NIH-PA Author Manuscript

ecdysis of insects injected with TcMet dsRNA as control insects ecdysed to pupae at 120 h after injection (not shown). Panels k–l show TcMet RNAi insects with adultoid characters upon incomplete larval-pupal ecdysis at 176 h after injection; k- dorsal view, l-ventral view; sclerotized antennae (k, blue arrow), pronotum (k, yellow arrow), forewings (k, red arrow), compound eyes (l- blue arrowhead), legs (l, green arrow) resembling adults; larval exuviae attached to abdomen are shown (k & l, black arrow). Panel m, ventral view of control insects at 176 h after injection showing gin-traps (blue arrowhead). Physical removal of larval cuticle from terminal abdominal regions of TcMet RNAi insects at 120 h after injection reveal pupal cuticle developed beneath larval skin (panel n) and at higher magnification pupal cuticle has gin-traps (panel o, blue arrowhead) and pupal urogomphi (o, black arrowhead). Scale Bar: 1 mm.

B & C. TcMet RNAi insects show adultoid characters. TcMet dsRNA was injected at 24 h AEFI and SEM images of insects at 176 h after injection (B) or at 120 h after injection (C) are shown. A) Middle panel show lateral view of TcMet RNAi phenotype and area of scanning of panels a–h are indicated. Panel a, ventral view of mouthparts; Lb-labium, Mx-maxillae, Mn-mandible; note the extension of mandibles (white star). Panel b, ommatidia of compound eyes (Ce). Panel c, antenna (at) with well-developed flagellar segments (white arrow). Panel d, short forewings (Fw) and well developed hindwings (Hw). Panel e, pro- & meso- thoracic legs with less differentiated tarsal segments (Ts) terminating in a pair of claws (Cl). Panel f, lateral view of abdominal region showing the attached larval exuvium (Lc), pupal cuticle (Pc) with gin-traps (Gt, white star). Panels g & h, larval exuviae physically removed from another insect injected with TcMet dsRNA showing similar phenotypes to reveal the development of male genital papillae (panel g, Mg) and pupal urogomphi (panel h, Ug). See text for details. Scale Bar: center panel – 200 μm; a,d,e,f,h – 100 μm; b,c,g – 50 μm. B) Panel a, larval cuticle physically removed from head, thoracic and terminal regions of abdomen to reveal the cuticle beneath the larval skin; Panels a–d, dorsal view; Lc- larval cuticle, Pc- pupal cuticle, Gt – gin-traps; note the cuticle of the head and thoracic regions are devoid of any cuticular structures. Dotted white lined squares in each panel indicate the area of scanning of corresponding panels (b–d). Panel b, abdominal region showing gin-traps (Gt) on the lateral margins of both sides. Panel c & d, closer view of gin-traps (Gt). Note the larval cuticle (Lc) has long setae (white arrow) and pupal cuticle (Pc) has short setae (white arrowhead) (Panel c). See text for details. Scale Bar: a,b – 200 μm; c,d – 100 μm.

NIH-PA Author Manuscript

NIH-PA Author Manuscript

NIH-PA Author Manuscript

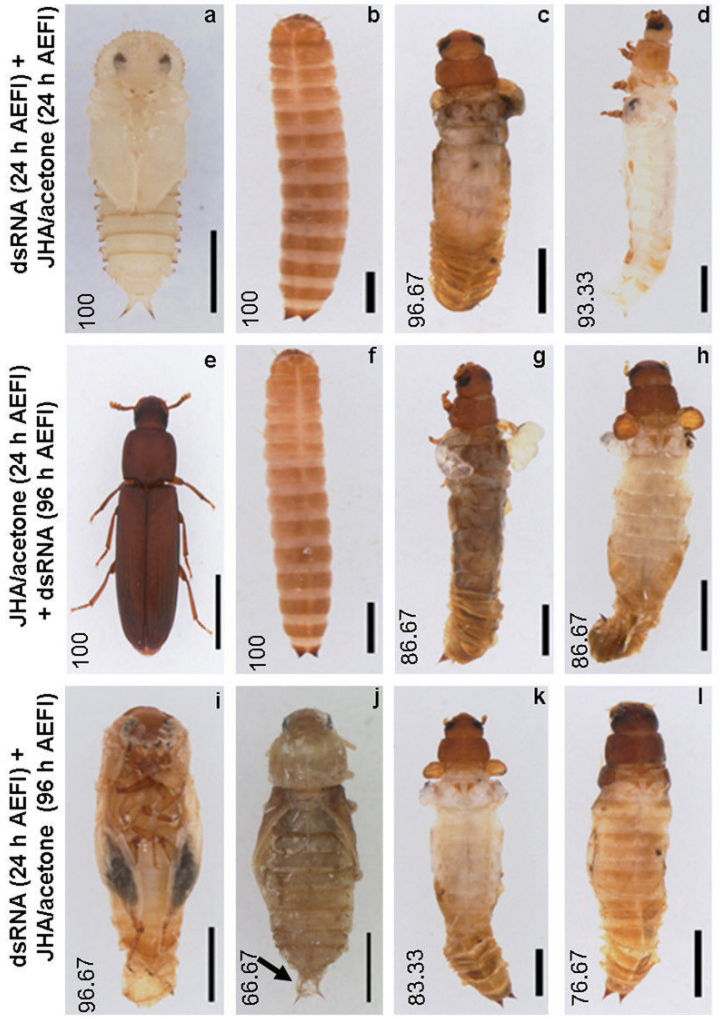

ds*malE*	+	+	-	-
dsmet	-	-	+	+
Acetone	+	-	+	-
Hydroprene	-	+	-	+

Fig. 4.

Depletion of TcMet mRNA confers resistance to hydroprene (JHA). Light micrographs of phenotypes after dsRNA injection and chemicals application (a–l). Three experimental groups are represented: Panels a–d, Panels e–h, Panels – i–l. The time of injection of dsRNA of TcMet or *malE* (control) and application of hydroprene (JHA), Hydroprene or acetone (control) are indicated on the left side of each group panels in a row. Numbers in each panel indicate the percentage of insects (n=30) showing the corresponding phenotypes. Table at the bottom indicate the type of dsRNA or chemical application received by insects in each corresponding columns. Black arrow in panel j indicates the presence of second pupal cuticle. See text for details. Scale bar: 1 mm.

NIH-PA Author Manuscript
NIH-PA Author Manuscript
NIH-PA Author Manuscript

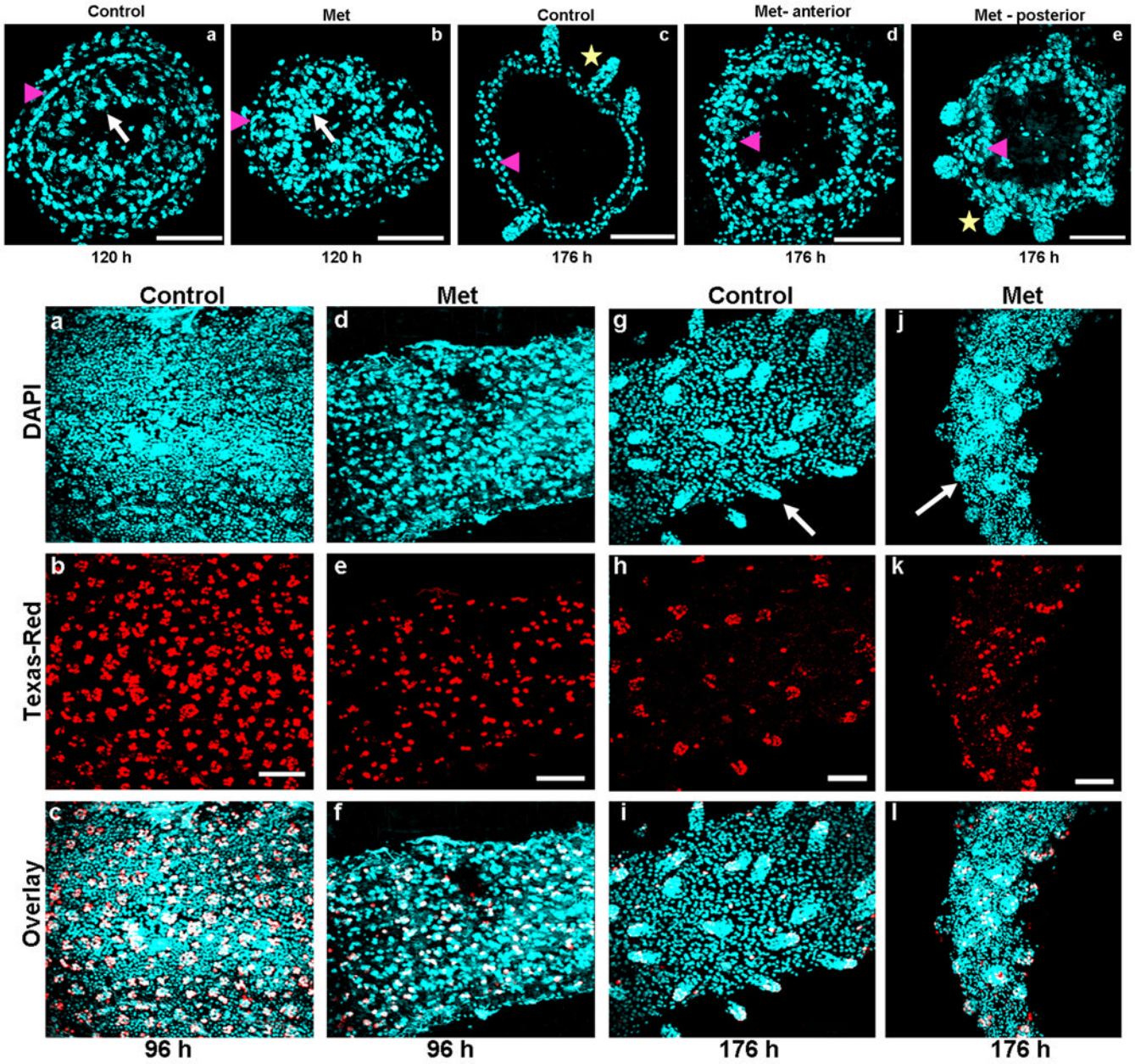

NIH-PA Author Manuscript
NIH-PA Author Manuscript
NIH-PA Author Manuscript

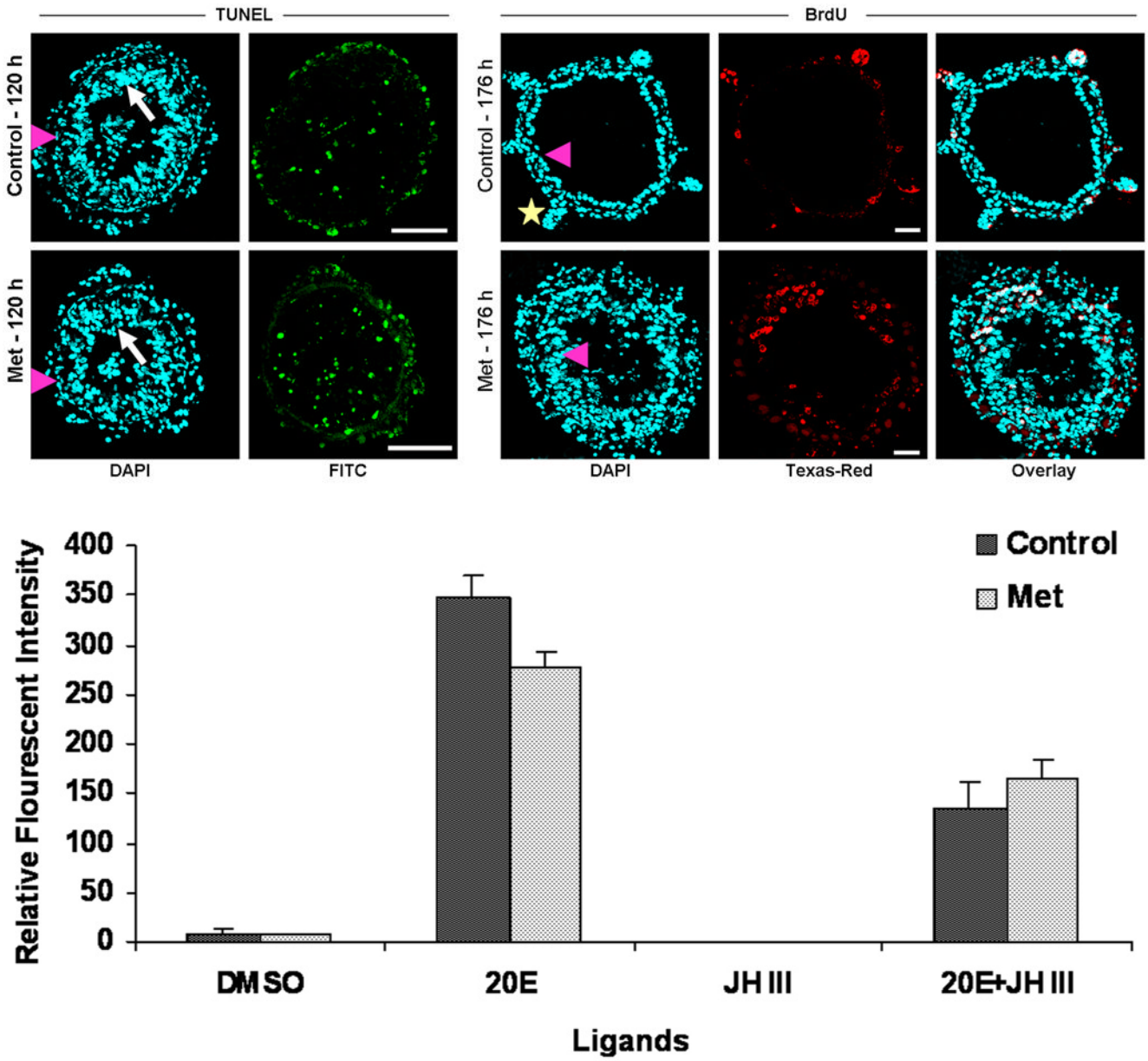

Fig. 5.

A. Midgut remodeling is not completely blocked in TcMet RNAi insects. Cross-sections of midguts (10 μm, thick) dissected from insects injected with TcMet or *malE* (control) dsRNA at 120 h (a & b), and 176 h (c–e) after injection are shown. Injections were done at 24 h AEFI. Nuclear staining is by DAPI (a–e); white arrow- polyploid larval cells, pink arrowhead – differentiating stem cells (a & b) or differentiated pupal gut epithelial cells (c–e), yellow star – crypts. At 120 h after injection, the morphology of midguts of both control and Tcmet RNAi insects looks similar (a & b) except for a small number of stem cells in TcMet RNAi insects (b). Note the arrangement of differentiating stem cells in a single layer representing the future pupal/adult gut epithelium is delayed in TcMet RNAi insects (b) when compared to control midguts (a). Panel a & b are representative image of the anterior and the posterior regions of midgut. At 176 h after injection, the representative cross-section of anterior and posterior regions of control midgut show well differentiated pupal gut epithelial cells and crypt formation

NIH-PA Author Manuscript

NIH-PA Author Manuscript

NIH-PA Author Manuscript

(c); while TcMet RNAi midguts show greater number of pupal gut epithelial cells; anterior region is devoid of crypts (d); posterior region has short crypt- like evaginations (e). Note that the crypt formation is delayed but not blocked or advanced in TcMet RNAi midguts. Scale Bar: 50 μm.

B. Effect of TcMet RNAi on stem cell proliferation at the posterior region of midgut. Z-stacks of whole-mounts of midgut dissected from TcMet or *malE* (control) dsRNA injected insects at 96 h and 176 h after injection are shown (a–l). Injections were done at 24 h AEFI. BrdU administration is done 12 h before dissection and the midguts are subjected to immunohistochemistry with anti-BrdU and Texas-Red conjugated secondary antibody. Panels show nuclear staining with DAPI (a,d,g,j), BrdU staining (b,e,h,k) and overlay of both (c,f,i.l). At 96 h after injection, smaller number of BrdU positive cells observed in TcMet RNAi midguts (e) when compared to control (b). Only stem cells or its immediate derivatives stain positive for BrdU (white) while other DAPI stained nuclei (blue) represent larval cells (c & f). Similar conditions are observed in the anterior region of midgut (not shown). At 176 h of injection, BrdU positive cells are concentrated only in crypt region of both control and TcMet RNAi insects (h & k). Note the difference in number of BrdU positive cells and size of crypts between control and TcMet RNAi midguts (g & j). The differentiated pupal gut epithelial cells do not stain positive for BrdU (blue in i & l). The anterior region of midgut is shown as cross-section in Fig 6C. Scale Bar: 20 μm.

C. TcMet RNAi does not block PCD of larval cells but delays the evagination of crypts in the anterior region of midgut. Cross-sections of midguts (10 μm, thick) dissected from TcMet and *malE* (control) dsRNA injected insects at 120 h after injection was subjected to TUNEL assay (a–d) and midguts dissected at 176 h after injection to BrdU assay (e–j). Injections were done at 24 h AEFI. For TUNEL assay, panels show nuclear staining by DAPI (a,c) and larval cells undergoing PCD detected by FITC-conjugated dUTP (b,d); white arrow – larval cells, pink arrowhead – stem cells, Note both control and TcMet RNAi midguts have TUNEL positive cells. For BrdU assay, panels show nuclear staining by DAPI (e, h), BrdU staining (f, i) and overlay (g, j). See Figure legend 6B for BrdU assay; pink arrowhead- differentiated pupal gut epithelial cells, yellow star – crypts. Note the BrdU positive cells are still in the proliferative state in the epithelium, a condition before evagination of crypts in TcMet RNAi midguts (i) while brdU positive cells are concentrated in the evaginated crypts of control midgut (f). Scale Bar: 50 μm.

D. Relative Florescence Intensity (RFI) of proliferating cells in *in vitro* cultured midguts dissected from insects injected with TcMet or *malE* dsRNA exposed to DMSO, 20E, JH III or 20E+JH III and quantified using BrdU labeling. Injections were done at 24 h AEFI. RFI were measured using Olympus Flouview software version 1.5. Squares of constant area (6662 mm^2) and length (26 mm) were drawn on composite Z-stack images. The average intensity in the marked area against the background was measured using the software. All other parameters (PMT, Gain, Offset, zoom) are the same for each image documented. Mean ± S.E. of three independent experiments (n=15) are shown.

NIH-PA Author Manuscript

NIH-PA Author Manuscript

NIH-PA Author Manuscript

Table 1

Phenotypes* of TcMet RNAi insects in comparison with control insects

Regions	Organs	TcMet RNAi insects	Control insects
Head	Antennae	well sclerotized; flagellar segments present; absence of sensillae	addition of flagellar segments; sclerotization of antennae and development of sensillae occur at pharate adult stage (72 – 96 h)
	Compound eyes**	several rows of photoreceptors (ommatidia)	formation of photorecpetors starts at the end of final instar (12–144 h AEFI); addition of rows progresses through pupal stage (0–96 h AEPS) till adult eclosion
	Mouthparts	well developed maxillary and labial palpi; overlapping of incisors of mandibles	development of palpi progresses through pupal stage; mandibles remain separated until 72 h AEPS; overlapping of incisors of mandibles occur at the end of pupal stage (96 h AEPS)
Thorax	Pronotum**	well developed and sclerotized; lack sensory bristles or setae	well developed with setae; unsclerotized in early pupae; sclerotization and formation of sensory bristles occur at pharate adult stage (72–96 h AEPS)
	Wings**	forewings short and sclerotized, hindwings normal and exposed	wings are formed during pupation (0 h AEPS); hindwing concealed beneath forewings always; sclerotization of forewings starts at 72 h AEPS and end at 6 h after adult eclosion
	Legs	Short; sclerotized; segmentation unclear; tarsi less differentiated; a pair of claws	differentiation of legs progresses throughout pupal stage (0–72 h AEPS) beneath the pupal skin; sclerotization of legs and well differentiated tarsi with a pair of claw seen only at the end of pharate adult stage (96 h AEPS)
Abdomen	Cuticle	unsclerotized; presence of short setae	pupal cuticle has short setae; unsclerotized
	Gin-traps	present	present only in pupal stage
	Urogomphi	well separated with no median; sclerotized at tips	well separated with no median; sclerotized at tips
	Genital papillae	well developed in both sexes	well developed in both sexes

* described based on the scanning and light micrographs

** structures observed well in advance beneath the uneclosed larval skin